The physical properties of cadmium telluride

A.J. Strauss

THE PHYSICAL PROPERTIES OF CADMIUM TELLURIDE (*)

A. J. STRAUSS

Lincoln Laboratory, Massachusetts Institute of Technology
Lexington, Massachusetts 02173, U. S. A.

Résumé. — Cet article passe en revue les propriétés structurales, thermiques, mécaniques, optiques et électriques du tellurure de cadmium. Celles-ci sont par ailleurs comparées aux propriétés physiques des autres composés IIB-VIA.

Abstract. — This paper reviews the structural, thermal, mechanical, optical, and electrical properties of CdTe and compares them with the physical properties of the other IIB-VIA compounds.

1. **Introduction.** — To introduce the papers that follow concerning specific properties and applications of CdTe, this paper gives a comprehensive survey of the whole range of physical properties of this material. A number of these properties will be compared with those of the other IIB-VIA compounds ; although care has been taken to insure that the information presented for the other compounds is accurate, it should be noted that this information has been drawn primarily from published compilations of data, whereas for CdTe a systematic attempt was made to select the most reliable values from the current literature. Most of the figures included are reproductions of figures from published papers. These have been chosen mainly because of their suitability as illustrations for a review article, and their selection does not imply any judgment concerning the overall merit of the papers in which they appear relative to other papers on the same subjects.

2. **Structural properties.** — Figure 1 shows a portion of the periodic table that includes the elements of Groups IIB and VIA. Both Cd and Te are located in the fourth row of the table, with atomic numbers of 48 and 52, respectively, so that CdTe belongs to the same isoelectronic series as Sn, InSb, and AgI. Since both HgSe and HgTe are semimetals, CdTe's average atomic number of 50 is the highest for any IIB-VIA semiconducting compound.

Table I lists the stable crystal structures at atmospheric pressure and the ionicities on the Phillips scale [1] of the 12 binary compounds formed by combining Zn, Cd, and Hg with O, S, Se, and Te. (For convenience, throughout the rest of the paper these will be referred to as the II-VI compounds, rather than the IIB-VIA compounds. The compounds of the Group IIA elements are not considered here.) Like ZnSe, ZnTe, HgSe and HgTe, as well as HgS above 377 °C and ZnS up to about 1 020 °C, bulk CdTe has the cubic zincblende structure, the binary analog of the diamond structure. In this structure each atom is tetrahedrally coordinated with four nearest neighbors of the other element. The hexagonal wurtzite structure of ZnO, CdS, CdSe, and of ZnS above its transition temperature, also exhibits tetrahedral coordination, which is characteristic of compounds with sufficiently covalent binding. The Phillips ionicity of CdTe is 0.717, the highest for any of the II-VI compounds with either zincblende or wurtzite structure at room temperature. Thus all the compounds of this type have ionicities less than 0.785, the value selected by Phillips as the threshold ionicity above which binary compounds are sufficiently ionic to have the octahedrally coordinated rocksalt structure. The only II-VI compound with rocksalt structure is CdO, whose ionicity is just 0.785.

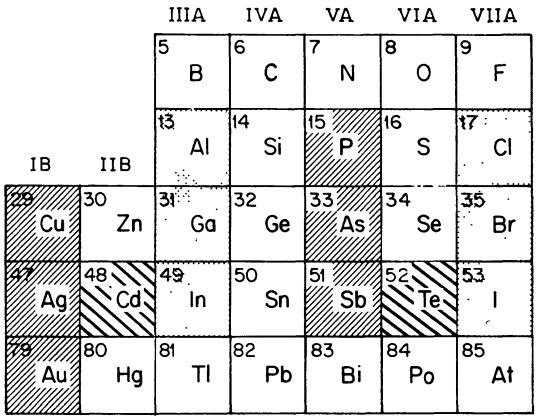

FIG. 1. — Portion of the periodic table including the elements of Groups IIB and VIA.

(*) This work was sponsored by the Department of the Air Force.

TABLE I

Some physical properties of the IIB-VIA compounds

Compound	Crystal structure [a]	Phillips ionicity [b]	Lattice constant (Å) [c]	Lattice mismatch with CdTe (%)	Energy gap at ~ 2 K (eV) [c]	Spin-orbit splitting (eV) [c]	Conductivity type
ZnO	W	0.616	$a = 3.250$ $c = 5.207$	− 29.1	3.435	− 0.005	n
ZnS	Z → W	0.623	5.409	− 16.5	3.839 (Z) 3.912 (W)	0.072 (Z)	n
ZnSe	Z	0.630	5.669	− 12.5	2.818	0.43	n, (p)
ZnTe	Z	0.609	6.103	− 5.8	2.391	0.93	p
CdO	R	0.785	4.695				n
CdS	W	0.685	$a = 4.137$ $c = 6.716$	− 9.7	2.583	0.066	n
CdSe	W	0.699	$a = 4.298$ $c = 7.016$	− 6.2	1.841	0.42	n
CdTe	Z	0.717	6.481	—	1.606	0.91	n, p
HgO	O, C		$a = 6.612$ $b = 5.520$ $c = 3.521$				
HgS	C → Z	0.79	$a = 4.146$ $c = 9.497$		2.090		
HgSe	Z	0.68	6.085	− 6.1	Semimetal	~ 0.45	n
HgTe	Z	0.65	6.460	− 0.3	Semimetal	~ 1.1	n, p

[a] Z = zincblende, W = wurtzite, R = rocksalt, C = cinnabar, O = orthorhombic.
[b] Ref. [1] [c] See *Physics and Chemistry of II-VI Compounds*, AVEN, M. and PRENER, J. S., Eds. (North-Holland, Amsterdam) 1967.

Figure 2 reproduces a photograph, published by Hilsum and Rose-Innes [2], of a model of the zincblende structure in which the atoms of one element are represented by black spheres and those of the other element by white spheres. The vertical direction in the photograph is parallel to a < 111 > axis. The model illustrates the tetrahedral configuration of nearest neighbors around each atom. It also shows that there are two types of { 111 } planes that alternate with each other, one consisting entirely of atoms of one element and the other consisting entirely of atoms of the other element, while the { 110 } planes contain equal numbers of the two kinds of atoms. As shown by the model, in which the uppermost layer consists of black spheres and the lowest layer of white spheres, the surfaces of a (111)-oriented sample are formed by planes of the two opposite types, so that one surface of a CdTe sample with this orientation consists of Cd atoms and the other of Te atoms. By convention, surfaces consisting of Group II atoms are designated as *A* surfaces and those consisting of Group VI atoms as *B* surfaces. The two types of surfaces have quite different chemical properties, as illustrated by figure 3, which

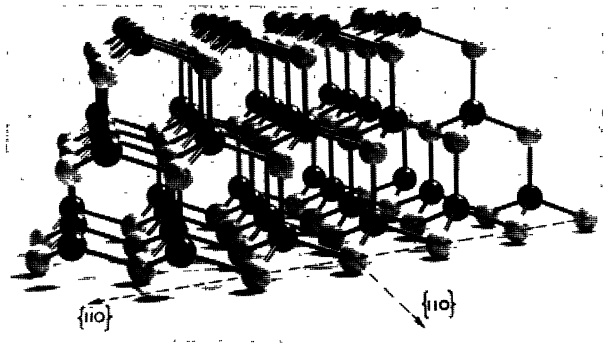

FIG. 2. — A model of the zincblende structure (Hilsum and Rose-Innes, Ref. [2]).

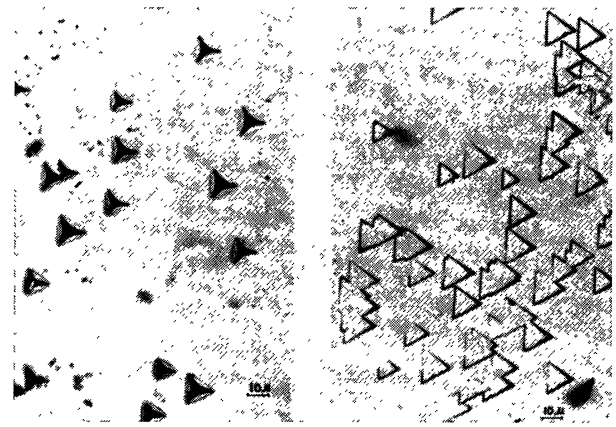

FIG. 3. — Etch pits on the { 111 } surface of CdTe. Left : A surface ; right : B surface (Inoue *et al.*, Ref. [3]).

shows the etch pits that Inoue, Teramoto, and Takayanagi [3] obtained by etching CdTe { 111 } surfaces with a solution containing nitric acid, silver nitrate, and potassium dichromate. The pits on both surfaces are triangular, with sides in < 110 > directions, but those on the *A* surface (shown on the left) are pyramidal or conical, while those on the *B* surface (shown on the right) are flat-bottomed.

Although the stable form of CdTe is the zincblende phase, which is always obtained for bulk samples at atmospheric pressure, thin films containing various proportions of the wurtzite phase can be prepared by vacuum deposition. Shalimova *et al.* [4] and Spinulescu-Carnaru [5] have reported that films with pure wurtzite structure are obtained by deposition on heated substrates when CdTe and metallic Cd are cœvaporated in an Ar atmosphere of 10^{-2} torr.

When bulk CdTe is subjected to high pressure, the zincblende form is transformed to the rocksalt structure at a transition pressure of 35 kbar [6, 7]. The variation in electrical resistance with pressure, as reported by Yu and Gielisse [7], is shown in figure 4.

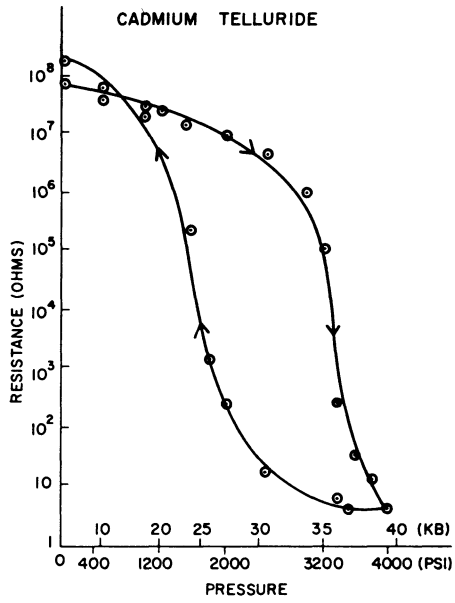

FIG. 4. — Electrical resistance of CdTe vs increasing and decreasing pressure (Yu and Gielisse, Ref. [7]).

With increasing pressure (upper curve) the resistance at first decreases gradually, then drops abruptly by about 6 orders of magnitude at the transition point. There is marked hysteresis when the pressure is reduced (lower curve), but the rocksalt phase is not retained at atmospheric pressure. The decrease in volume accompanying the zincblende-to-rocksalt transformation is reported by Mariano and Warekois [8] and by Cline and Stephens [6] to be between 15 and 20 %. Both CdS and CdSe also transform to conducting rocksalt phases at high pressures, while HgSe, and HgTe are transformed to the cinnabar structure. Samara and Drickamer [9] report transitions of ZnS, ZnSe, and ZnTe to conducting phases of unknown structure at pressures exceeding 100 kbar.

The lattice constants of the II-VI phases stable at room temperature and atmospheric pressure are listed in table I, together with the percentage differences in lattice constant between CdTe and the compounds with zincblende and wurtzite structures. The most probable value for the lattice constant of CdTe is 6.481 Å. Although Medvedev *et al.* [10] have reported a systematic dependence of lattice constant on carrier concentration for single-crystal samples, with values as high as 6.484 Å measured for high-resistivity specimens, no such variation was observed in similar experiments by Vaipolin and Rud' [11], who obtained values of 6.481 8 ± 0.003 Å. Cadmium telluride has the largest lattice constant of any II-VI compound. Because the difference between the constants for CdTe and HgTe is only 0.3 %, high-quality epitaxial layers of $Hg_{1-x}Cd_xTe$ solid solutions covering the entire alloy composition range can be grown on CdTe substrates [12].

The structural properties of CdTe at 300 K are summarized in table II. Crystals can be cleaved quite readily on the { 110 } planes. The value listed for the shortest Cd-Te distance, 2.806 Å, was calculated on the assumption that CdTe has the ideal zincblende structure. From a structure-factor analysis of the measured intensities of x-ray diffraction lines, Vaipolin [13] has concluded that the Cd atoms are displaced along the < 111 > directions from their ideal positions, so that each Cd atom is at a distance of 2.775 Å from three of the neighboring Te atoms and 2.908 Å from the fourth.

TABLE II

Structural properties of CdTe *at* 300 K

Crystal structure	Zincblende
Space group	$F\bar{4}3m$
Cleavage plane	{ 110 }
Molecules per unit cell	4
Molecular weight (g)	240.00
Lattice constant (Å)	6.481
Shortest Cd-Te distance (Å)	2.806
Molar volume (cm^3)	40.99
Conc. of Cd sites (cm^{-3})	1.469×10^{22}
X-ray density (g cm^{-3})	5.855

3. **Thermal and mechanical properties.** — The linear thermal expansion coefficient of CdTe, $\alpha \equiv (1/l)(dl/dT)$, is (4.9 ± 0.1) 10^{-6} K^{-1} at room temperature and increases with increasing temperature [14, 15]. Williams, Tomlinson, and Hampshire [14] report that at 420 °C $\alpha = 5.67 \times 10^{-6}$ K^{-1} and the lattice constant is 6.495 5 Å, compared with 6.480 9 Å at room temperature. Below room temperature α

decreases, becoming negative at 62 ± 2 K, as shown in figure 5. The circles represent the data of Greenough and Palmer [16] for a single crystal measured along a < 100 > axis, the crosses and triangles those of other

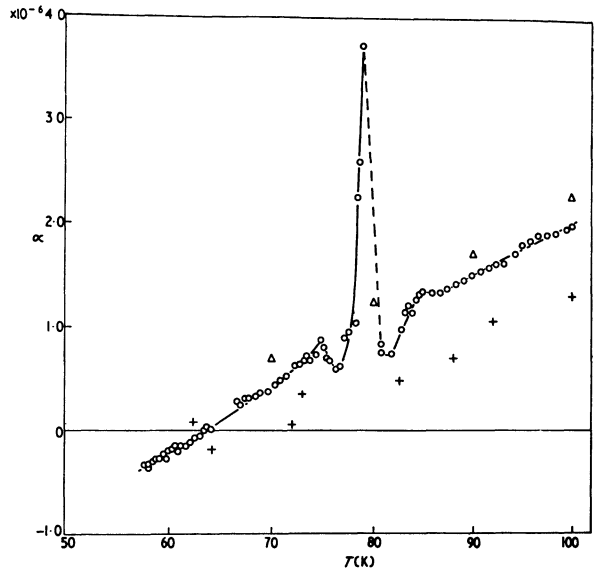

FIG. 5. — Linear thermal expansion coefficient of CdTe vs temperature (Greenough and Palmer, Ref. [16]).

authors for polycrystalline samples. The strong anomaly found by Greenough and Palmer, which peaks at 79 K, was not confirmed in subsequent single-crystal measurements by Smith and White [15]. The fact that the anomaly occurs very close to liquid nitrogen temperature seems somewhat suspicious.

As the temperature is decreased below 60 K, α initially becomes more and more negative. As shown in figure 6, where the data of Smith and White

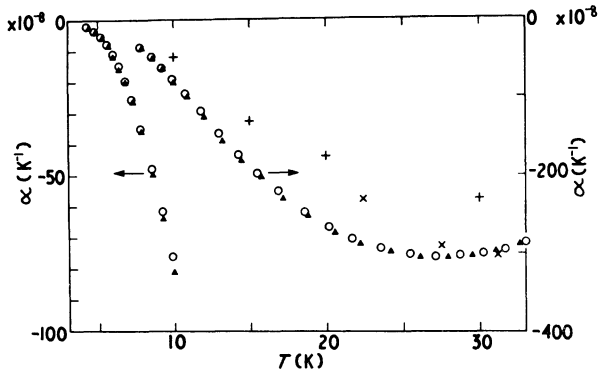

FIG. 6. — Linear thermal expansion coefficient of CdTe vs temperature (Smith and White, Ref. [15]).

[15] are represented by the circles and triangles and those of other authors by the crosses and x's, α reaches a maximum negative value of about -3.0×10^{-6} K^{-1} at 27 K. It then decreases in magnitude but remains negative down to absolute zero. Negative expansion coefficients are also exhibited by other zincblende-structure compounds at low temperatures, but CdTe represents an extreme case, as shown by the results of Smith and White [15] for Ge, GaAs, ZnS, ZnSe, and CdTe given in figure 7. In this figure the

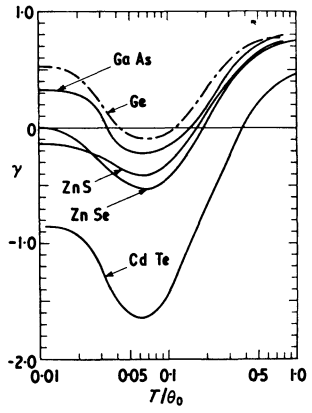

FIG. 7. — Grüneisen parameter vs reduced temperature for crystals with diamond or zincblende structure (Smith and White, Ref. [15]).

Grüneisen parameter γ is plotted against the reduced temperature relative to the Debye temperature. This parameter is proportional to α times the product of the molar volume and bulk modulus divided by the specific heat, and it therefore has the same sign as α.

Figure 8 shows the thermal conductivity κ measured by Slack [17] between 3 and 300 K for single-crystal

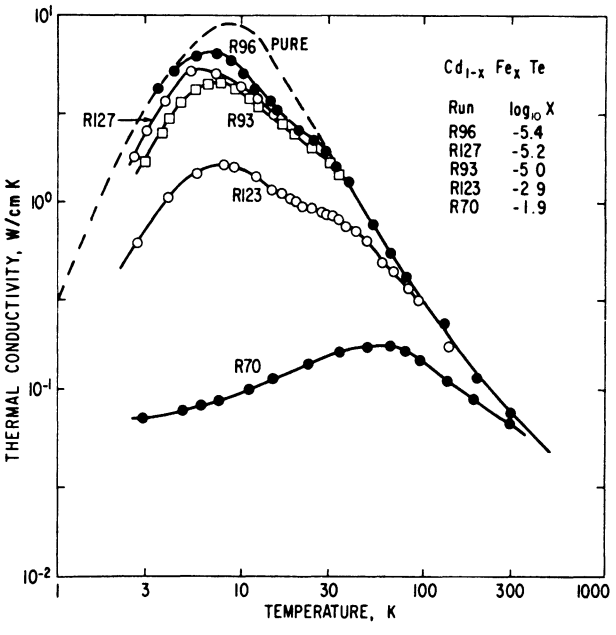

FIG. 8. — Thermal conductivity of Fe-doped CdTe vs temperature (Slack, Ref. [17]).

samples of CdTe containing various amounts of Fe. For these samples the electronic contribution to κ is insignificant compared to the lattice phonon contribution. The strong, structured decrease in κ with increas-

ing Fe concentration is attributed by Slack to resonant phonon scattering resulting from the absorption of phonons to produce electronic transitions among the 5 low-lying d-shell levels of the isolated Fe^{2+} ions. Since even his purest sample contained enough Fe to cause appreciable scattering, Slack estimated the curve labelled *pure* on the basis of the κ-vs-T curves for the other II-VI compounds, all of which exhibit a characteristic maximum at low temperature. Sood, Singh, and Verma [17A] obtained a theoretical curve that is in reasonable agreement with the *pure* curve (although their curve was fitted to Holland's earlier experimental data [17B], since it was published prior to Slack's paper) by summing the separate contributions to the conductivity that they calculated for the transverse and longitudinal acoustic phonons.

The thermal conductivity at 300 K for CdTe, 0.075 W cm^{-1} K^{-1}, is the lowest for any of the tetrahedrally coordinated II-VI compounds except HgSe and HgTe. The values for these and several other materials are shown in figure 9, which is a plot given by

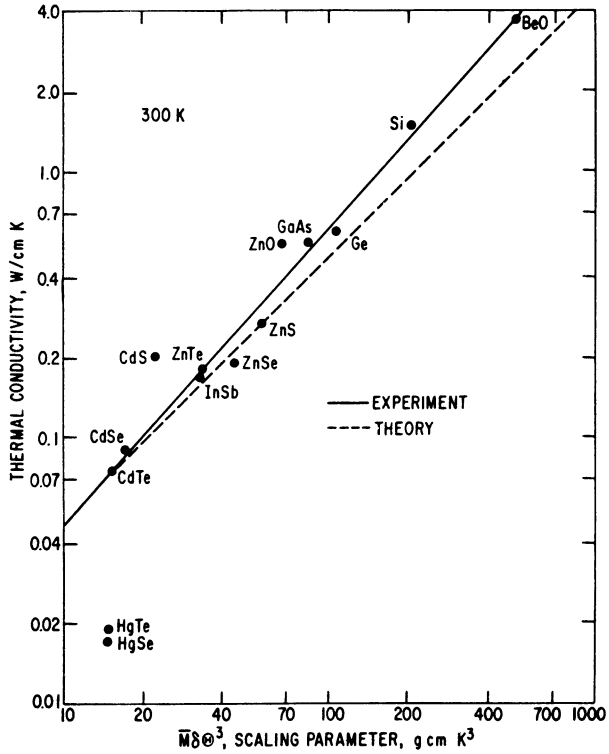

FIG. 9. — Thermal conductivity vs scaling parameter for crystals with tetrahedrally coordinated structures (Slack, Ref. [17]).

Slack [17] of κ at 300 K as a function of the scaling parameter $\overline{M}\delta\theta^3$, where $\overline{M}$ is the average atomic mass, δ is the cube root of the average volume per atom, and θ is the Debye temperature at absolute zero. All the points fall close to a straight line except those for HgSe and HgTe, which have conductivities only about 25 % as high as expected.

The thermal and mechanical properties of CdTe at 300 K are summarized in table III. The heat capacity

TABLE III

Thermal and mechanical properties of CdTe *at* 300 K

Linear expansion coeff. (K^{-1}) ([a])	$(4.9 \pm 0.1) \times 10^{-6}$
Thermal conductivity (W cm^{-1} K^{-1}) ([b])	0.075
Heat capacity, C_p (cal g-atom^{-1} K^{-1}) ([c])	5.9
Isothermal compressibility (kbar^{-1}) ([d])	3.96×10^{-3}
Elastic constants ([e])	
C_{11}(N m^{-2})	$(5.35 \pm 0.03) \times 10^{10}$
C_{12}(N m^{-2})	$(3.70 \pm 0.05) \times 10^{10}$
C_{44}(N m^{-2})	$(2.02 \pm 0.03) \times 10^{10}$
Microhardness (kp mm^{-2}) ([f])	55 to 140

([a]) Refs. [14, 15].
([b]) Ref. [17].
([c]) Ref. [18].
([d]) Ref. [6].
([e]) Refs. [16, 19, 20].
([f]) Ref. [22].

value, 5.9 cal g-atom^{-1} K^{-1}, was read off the curve of C_p vs T published by Rusakov, Vekilov, and Kadyshevich [18]. The range of values given for each of the elastic constants includes the results given by McSkimin and Thomas [19], Vekilov and Rusakov [20] and Greenough and Palmer [16].

The variation of these constants with temperature was determined both by Vekilov and Rusakov and by Greenough and Palmer. Their results for 77 K are in good agreement with each other but not with the earlier data of Berlincourt, Jaffe, and Shiozawa [21] at this temperature. The range of microhardness values listed in table III was observed by Swaminathan, Selim, and Kröger [22] in measurements made in the dark on In-doped samples that had been annealed at various temperatures and Cd pressures. They found that the dark values increased with increasing carrier concentration, while the microhardness could be either increased or decreased by illumination, depending upon the annealing conditions. Changes in the mechanical properties of CdTe with carrier concentration and illumination have also been observed by Carlsson and Ahlquist [23] who found that the yield stress in compression increased with increasing carrier concentration for both n- and p-type samples and that the yield stress and crack propagation were both increased by illumination. They attributed the latter effects to a light-induced decrease in mobile dislocation density.

Values of the Debye temperature θ_D for CdTe have been obtained from several types of experimental data. Analyses of x-ray diffraction intensity data for 96 to 300 K by Walford and Schœffel [24] and for 281 to 608 K by Zubik and Valvoda [25] show that over these intervals the x-ray Debye temperature is close to 140 K, essentially independent of temperature. Birch [26] has determined the temperature dependence of θ_D between 1.8 and 25 K from heat capacity data over this range. He obtained a limiting value of 160 ± 2 K for θ_D at absolute zero, in very good agreement with the values of 161 ± 4 and 162.7 K found

by Vekilov and Rusakov [20] and by Greenough and Palmer [16], respectively, by extrapolating elastic constant data to absolute zero. The Debye temperatures of the tetrahedrally coordinated II-VI compounds are compared in figure 10, which is a plot given by

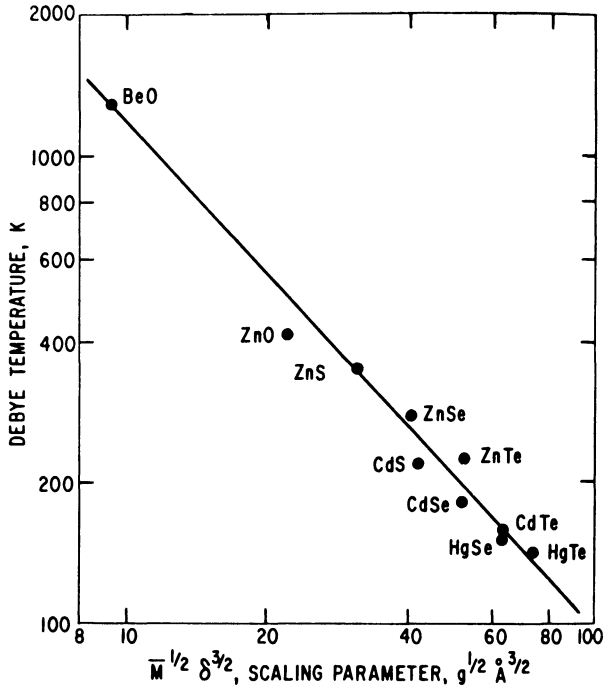

FIG. 10. — Debye temperature vs scaling parameter for tetrahedrally coordinated II-VI compounds (Slack, Ref. [17]).

Slack [17] of θ_D at absolute zero as a function of the scaling parameter $(\bar{M}\delta^3)^{1/2}$, where $\bar{M}$ and δ have the same significance as above. The only compounds with Debye temperatures lower than that of CdTe are HgSe and HgTe.

All the thermal and mechanical properties of a material depend ultimately on its normal modes of vibration, as represented by the phonon dispersion relation. A determination of this relation for CdTe at 300 K has been made by Rowe *et al.* [27] by means of neutron inelastic scattering measurements. Their results are shown in figure 11, which gives the phonon frequencies as a function of the reduced wave vector, $\zeta = aq/2\pi$, for the [100], [111], and [110] directions of

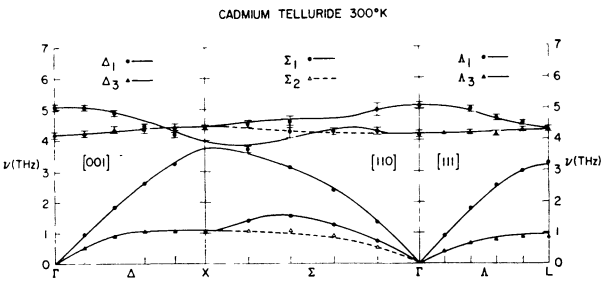

FIG. 11. — Phonon dispersion relation for CdTe (Rowe *et al.*, Ref. [27]).

propagation. The letters Γ, X and L refer to the symmetry points at the center of the Brillouin zone, the (100) zone boundary, and the (111) zone boundary, respectively. The symbols in the figure represent the experimental values for the longitudinal optical, transverse optical, longitudinal acoustic, and transverse acoustic phonons, while the solid lines represent the calculated results obtained by fitting a 14-parameter shell model to the experimental data for the elastic constants, static and high-frequency dielectric constants, and piezoelectric constant of CdTe, as well as the phonon frequencies. Plumelle and Vandevyver [28] have recently used an 11-parameter rigid-ion model to fit the elastic constant and phonon frequency data. Table IV lists the phonon frequencies

TABLE IV

Symmetry-point phonon frequencies (THz) *in* CdTe *at* 300 K ([a])

Phonon branch	Γ	X	L
LO	5.08	—	4.33
TO	4.20	4.44	4.33
LA	0	—	3.25
TA	0	1.05	0.88

([a]) Ref. [27].

measured by Rowe *et al.* [27] at Γ, X and L. They note that the values for the longitudinal and transverse optic modes of 5.08 and 4.20 THz, respectively, are in good agreement with the values of 5.03 and 4.22 THz obtained by Perkowitz and Thorland [29] from far-infrared reflectivity data for n-type CdTe.

4. **Optical properties.** — We will now turn our attention to the interaction of CdTe with electromagnetic radiation, first considering γ-rays and then optical photons. Figure 12, which reproduces a plot given by Serreze *et al.* [30] shows the γ-ray absorption coefficients calculated for CdTe, Ge, and Si over the photon energy range from 20 to 2000 keV. For Si up to about 30 keV and for CdTe and Ge up to about 100 keV, the total absorption is essentially equal to the absorption due to the photoelectric effect (curves labelled PE), which is highest for CdTe because it has the highest atomic number of the three materials — an average of 50, compared with 32 for Ge and 14 for Si. With increasing energy, as the cross section for the photoelectric effect decreases, absorption due to Compton scattering becomes increasingly important and eventually dominant. Gamma rays that initially undergo Compton scattering may then generate carriers by the photoelectric effect. Siffert *et al.* [31] have reported that in one series of experiments this multiple process contributed about half the counts forming the full-energy photoelectric peak.

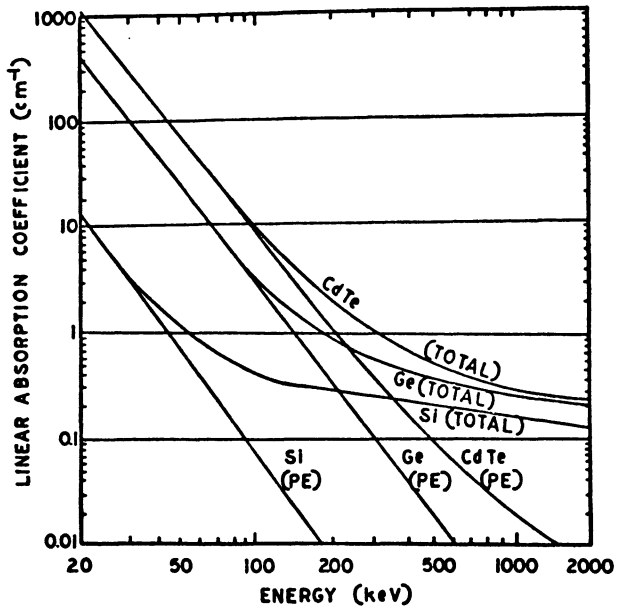

FIG. 12. — Gamma-ray absorption coefficients vs photon energy for CdTe, Ge, and Si (Serreze *et al.*, Ref. [30]).

Figure 13 shows the temperature dependence reported by Alberigi Quaranta *et al.* [32] for the energy loss associated with the production of one electron-hole pair in CdTe by ionizing radiation. The data were

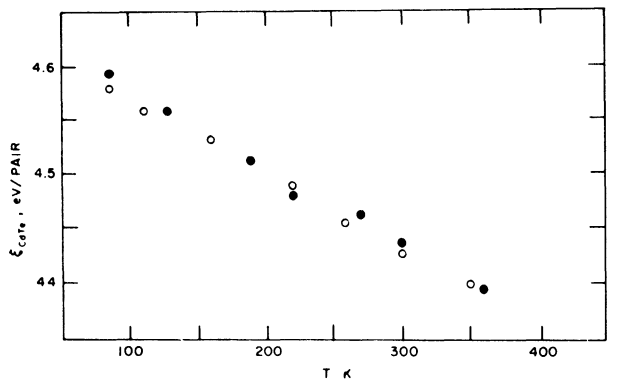

FIG. 13. — Energy loss associated with production of electron-hole pairs in CdTe as a function of temperature (Alberigi Quaranta *et al.*, Ref. [32]).

obtained by measurements on semi-insulating samples in which 5.477 MeV alpha particles from ^{241}Am were used to generate the carrier pairs. It is assumed that the same energy per pair is required for generation by γ-rays. The value measured at 300 K was 4.43 eV, in very good agreement with the value of 4.46 eV obtained by Cornet *et al.* [33] in measurements on surface-barrier detectors fabricated from low-resistivity (10-200 Ω.cm) n-type CdTe. The agreement at 77 K is not as good, with values of 4.58 and 4.75 eV obtained by Alberigi Quaranta *et al.* [32] and Cornet *et al.* [33], respectively.

The interactions of optical photons with a semiconductor, unlike those of high-energy ionizing radiation, are determined by the details of the semiconductor's electronic and mechanical properties. We may distinguish three regimes of photon energy with different characteristic optical absorption mechanisms. For photon energies greater than the semiconductor energy gap E_g there are very strong absorptions due to excitation of electrons from the valence bands or atomic core levels to the conduction bands and, for sufficiently high energies, due to photoemission from the valence bands or core levels to vacuum. For photon energies less than E_g but greater than about twice the longitudinal optical phonon energy the absorption is relatively weak, resulting primarily from interactions with free carriers, electronic levels within the bandgap, localized vibrational modes due to impurities, or defects such as precipitates. Finally, for sufficiently low photon energies the absorption again increases due to photon-phonon interactions.

The absorption is so intense at above-bandgap energies, with absorption coefficients generally exceeding 10^4 cm^{-1}, that transmission measurements are impracticable. Therefore reflectance techniques are used to elucidate the details of the valence and conduction band structures. Figure 14 shows the energy band

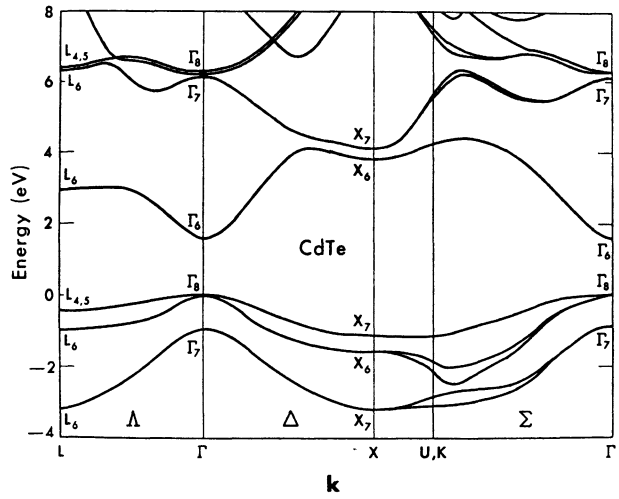

FIG. 14. — Calculated energy band structure of CdTe (Chadi *et al.*, Ref. [34]).

structure of CdTe calculated by Chadi *et al.* [34] who used the empirical pseudopotential method to fit their reflectance data as well as other experimental results. As in other II-VI semiconductors with the zincblende or wurtzite structure, the lowest conduction band edge and highest valence band edge are both at Γ, so that the energy gap is direct. The bandgap is 1.606 eV at liquid helium temperatures, and the spin-orbit splitting between the valence bands at Γ is 0.91 eV. The second-lowest conduction band edge is located at the L-point, 1.35 eV above the lowest.

The degree of agreement between the calculated band structure and experimental data is illustrated by figure 15, which compares the reflectance calculated from the band structure with the experimental values

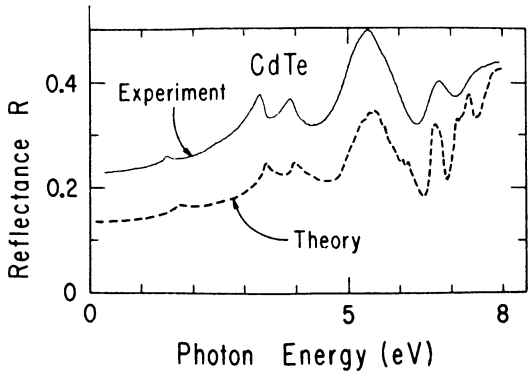

FIG. 15. — Experimental and theoretical curves for reflectance of CdTe vs photon energy (Freeouf, Ref. [35]).

measured at 300 K by Freeouf [35], who used a tungsten source at energies below 4.5 eV and synchrotron radiation at higher energies. The theoretical curve closely reproduces the structure in the experimental curve, but its absolute magnitude is considerably lower.

The energy gaps of the II-VI compounds at liquid helium temperatures, together with the spin-orbit splittings of the valence bands at Γ, are summarized in table I. The energy gap of CdTe is the lowest for any of the compounds except HgSe and HgTe, which are semimetals with zero or possibly negative energy gaps.

For a direct-gap semiconductor, the optical absorption coefficient decreases abruptly when the photon energy is reduced below E_g. Figure 16 shows the absorption edge data obtained by Marple [36] at several temperatures for single-crystal samples that were first measured after being mechanically polished, then chemically polished and remeasured. These results show that mechanical damage significantly increases the lower absorption coefficients and leads to marked curvature of the absorption edge. This effect probably

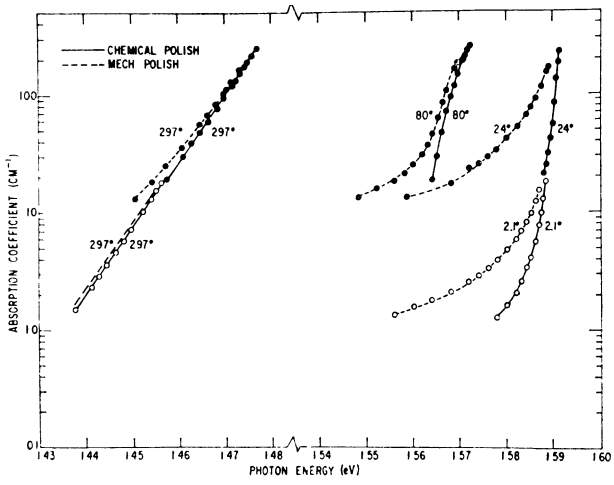

FIG. 16. — Optical absorption edge of CdTe vs temperature (Marple, Ref. [36]).

explains why early workers interpreted their data as evidence for an indirect energy gap in CdTe.

Figure 16 also shows that E_g for CdTe shifts to lower values with increasing temperature, the temperature dependence exhibited by most semiconductors. This shift is shown more clearly by Marple's complete data between 2 and 177 K, as given in figure 17. Because of the complexities of the absorption process, which involves phonon absorption and exciton formation, these data cannot be used for an accurate determination of the temperature dependence of E_g. Up to about 150 K, however, this dependence can be determined from reflectance and piezoreflectance spectra, which exhibit sharp structure that makes it possible to evaluate the exciton energy and therefore E_g. The reflectance data of Thomas [37] and of Marple [38] show that as the temperature is increased from liquid helium temperature E_g decreases very slowly up to about 20 K, then begins to decrease more rapidly, and between 80 and 150 K decreases linearly at the rate of -3.5×10^{-4} eV K^{-1}. Extrapolation to 300 K gives $E_g = 1\,520$ eV, in rather good agreement wit the value of 1.529 eV obtained by Camassel *et al.* [39] by extra-

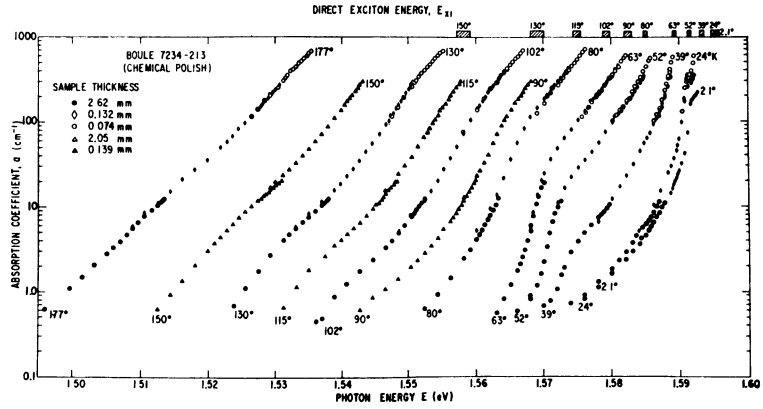

FIG. 17. — Optical absorption edge of CdTe vs temperature (Marple, Ref. [36]).

polating their piezoreflectance results for the interval between 77 and 145 K. According to Loferski's theoretical calculations [40], an energy gap of 1.52 eV is very close to the value that can potentially yield the maximum possible efficiency for the conversion of solar radiation to electric power by means of semiconductor photovoltaic solar cells.

Electroreflectance techniques have been used by Babonas, Bendoryus and Shileika [41] and by Melz and Ortenburger [42] to determine the effect of hydrostatic pressure on the energy gap and spin-orbit splitting at Γ for CdTe. Their results are in good agreement. For the pressure coefficient of E_g at room temperature they obtained 7.9×10^{-6} and 8.3×10^{-6} eV/bar, respectively, and for the pressure coefficient of the spin-orbit splitting they obtained 0.8×10^{-6} eV/bar at 300 K and 0.7×10^{-6} eV/bar at 77 K, respectively.

For photon energies between the absorption edge and the onset of lattice phonon absorption — corresponding to wavelengths between about 0.9 and 30 μm — the optical absorption of CdTe results primarily from the interaction between photons and various types of defects, if free carriers are regarded as electronic defects. Figure 18 shows the data of Strauss

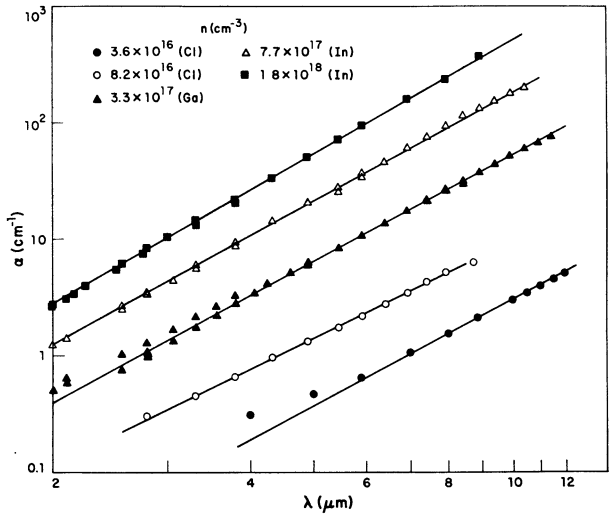

FIG. 18. — Free-carrier absorption of n-type CdTe at 300 K (Strauss and Iseler, Ref. [43]).

and Iseler [43] for the free-carrier absorption as a function of wavelength λ measured at 300 K for single-crystal n-type samples with electron concentrations between 3.6×10^{16} and 1.8×10^{18} cm^{-3}. For a given concentration, the absorption coefficient exhibits the λ^m dependence characteristic of intraband free-carrier absorption, with values of m ranging from 2.7 to 3.4 rather than the classical Drude square-law dependence. The absorption cross section at 10.6 μm, the wavelength of the CO_2 laser, is 1.0×10^{-16} cm^2 for the lowest concentration sample and increases to 3.5×10^{-16} cm^2 for the highest concentration sample.

Jensen [44] has obtained a very good theoretical fit, without using any adjustable parameters, to the data for concentrations of 1.4×10^{17} cm^{-3} and below. According to her calculations, in this concentration range polar optical mode scattering is the predominant scattering mechanism, while ionized impurity scattering makes a very small contribution.

The optical absorption of p-type CdTe samples at photon energies less than E_g has been measured by Vul *et al.* [45] and by Capek *et al.* [46]. Figure 19 shows

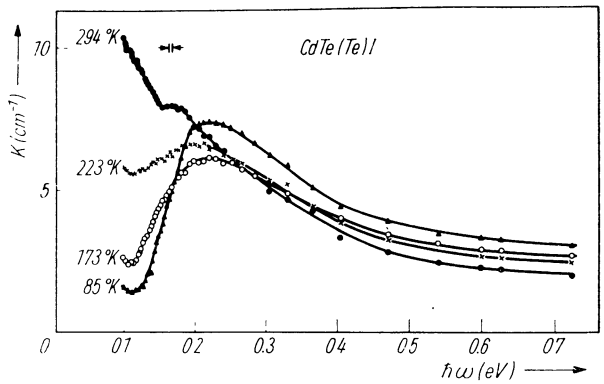

FIG. 19. — Optical absorption of p-type CdTe vs wavelength (Capek *et al.*, Ref. [46]).

the results of Capek *et al.* for a nominally undoped sample grown in the presence of excess Te, which had a hole concentration of 3.2×10^{16} cm^{-3} at 300 K that decreased by several orders of magnitude on cooling to 80 K. The absorption peak at about 0.2 eV, which is not strongly temperature dependent, is attributed to transitions from the valence band to an acceptor level, while the temperature-dependent absorption at lower energies is attributed to interband free-carrier transitions from the light-hole valence to the heavy-hole valence band. At room temperature the absorption cross section at 10.6 μm (0.12 eV) is about 3×10^{-16} cm^2, and similar values were found for other samples by both Capek *et al.* [46] and Vul *et al.* [45]. In P-doped samples the former authors observed absorption peaks at 0.07 and 1.07 eV that they attributed to transitions to the P acceptor level from the doubly-degenerate and split-off valence bands, respectively.

For sufficiently small photon energies, optical absorption due to interactions with the lattice phonons becomes significant. The onset of lattice absorption in CdTe is shown by figure 20. This figure gives the data of Deutsch [47] for the absorption coefficients of CdTe, ZnSe, and GaAs as a function of the reduced frequency, defined as the ratio of photon frequency ω to the longitudinal optical phonon frequency ω_{10}, which is 168 cm^{-1} for CdTe. According to the CdTe data, as represented by the solid curve, the absorption coefficient is 0.01 cm^{-1} at about 21 μm.

The point shown in figure 20 at 6×10^{-4} cm^{-1}

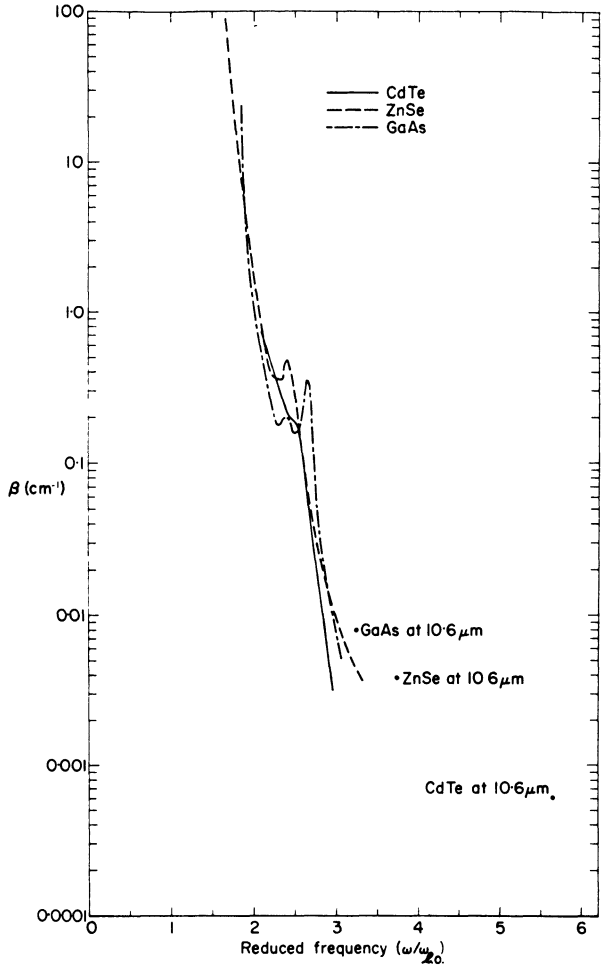

FIG. 20. — Lattice absorption of CdTe vs reduced photon frequency (Deutsch, Ref. [47]).

represents the lowest absorption coefficient at 10.6 μm that had been observed for CdTe at the time Deutsch submitted his paper. To the best of my knowledge, the lowest reported value is 2.5×10^{-4} cm^{-1}. It is obvious that extrapolation of the linear portion of the CdTe curve would yield an absorption coefficient at 10.6 μm many orders of magnitude below 10^{-5} cm^{-1}, indicating that lattice absorption is not the mechanism that is currently setting the lower limit on the transmission of CdTe at this wavelength. It also appears that free-carrier absorption is not the limiting mechanism, since several groups have reported the preparation of semi-insulating CdTe with hole concentrations of less than 10^{10} cm^{-3}, which would give absorption coefficients well below 10^{-5} cm^{-1} if the measured free-carrier cross sections were maintained. Instead, it seems probable that microstructural defects such as precipitates, dislocations, and stacking faults are responsible for the absorption at 10.6 μm. In a study utilizing transmission electron microscopy. Magee, Peng, and Bean [48] have shown a correlation between the concentration of such defects and the absorption coefficient for coefficients down to 10^{-4} cm^{-1}.

The absorption data for CdTe plotted in figure 20 extend only to about 330 cm^{-1}, corresponding to 30 μm. As the photon energy is decreased still further, the absorption becomes structured and much more intense. Figure 21 shows the transmittance data

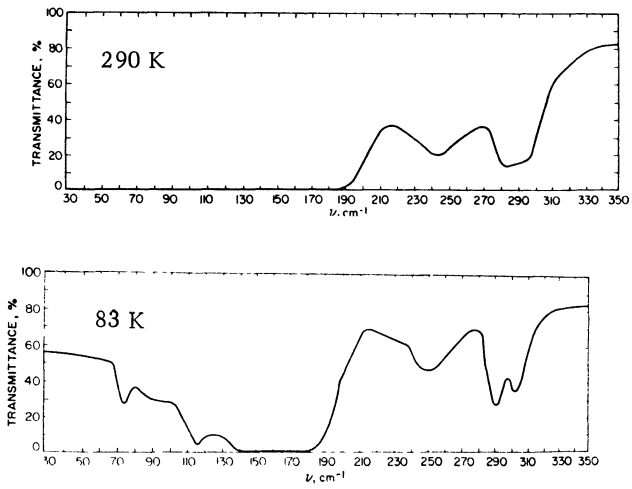

FIG. 21. — Lattice absorption of CdTe vs photon frequency (Stafsudd *et al.*, Ref. [49]).

obtained by Stafsudd, Haak, and Radisavljevic [49] for a sample 0.45 mm thick over the frequency range from 30 to 350 cm^{-1}, corresponding to wavelengths from about 28 to 330 μm. The upper curve was measured at 290 K, the lower at 83 K. The strongest absorption occurs at the fundamental of the transverse optical mode, 141 cm^{-1}, while the other peaks are two-phonon combination bands. Table V lists the 6 strongest peaks and the phonon assignments given by Danielewicz and Coleman [50].

TABLE V

Strongest lattice absorptions in CdTe ([a])

Approximate frequency (cm^{-1})	Approximate wavelength (μm)	Phonon assignment
72	138	2 TA
115	88	LO − TA
141	70	TO
250	40	LO + LA
290	34.5	LO + TO
300	33.1	2 LO

([a]) Ref. [50].

Figure 22 shows the data of Manabe, Mitsuishi, and Yoshinaga [51] for the reflectivity of CdTe and several other II-VI compounds between 20 and 100 μm. The characteristic restrahlen band associated with the transverse optical phonon has its peak at about 67 μm

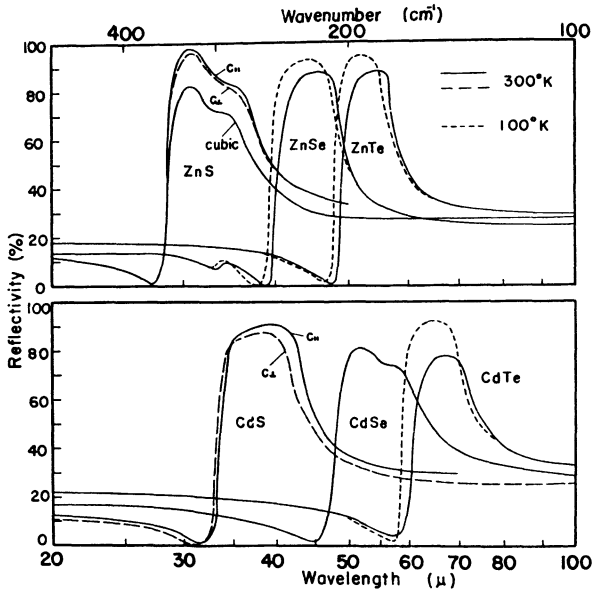

FIG. 22. — Far-infrared reflectivity of IIA-VIB compounds (Manabe *et al.*, Ref. [51]).

for CdTe at 300 K, the longest wavelength for any of the compounds investigated. Numerous authors have analyzed reflectivity data for CdTe in terms of a classical oscillator model to obtain values for the static and high-frequency dielectric constants. These constants are listed in table VI, together with some other

TABLE VI

Some optical properties of CdTe *at* 300 K

Refractive index, n_0, at 10.6 μm [a]	2.672
Reflectivity at 10.6 μm [b]	0.207
$(1/n)\ dn/dT\ (K^{-1})$ [c]	$(4.4 \pm 0.03) \times 10^{-5}$
Dielectric constants [d]	
Optical, ε_∞	7.15 ± 0.05
Static, ε_0	10.3 ± 0.1
Damping constant, $\Gamma\ (cm^{-1})$ [d]	7.5 ± 1.2
Elastooptic coefficients [e]	
p_{11}	-0.152 ± 0.013
p_{12}	-0.017 ± 0.011
p_{44}	-0.057 ± 0.007

[a] See Ref. [50].
[b] Calculated from n_0.
[c] KIEFER, J. E. and YARIV, A., *Appl. Phys. Lett.* **15** (1969) 26.
[d] See Refs. [29] and [50].
[e] WEIL, R. and SUN, M. J., Proc. Int. Sym. on Cadmium Telluride, Strasbourg, 1971.

optical properties of CdTe, while table VII gives values of the electrooptic coefficient r_{41} and the nonlinear susceptibility. Since the electrooptic coefficient of CdTe at 10.6 μm is about 4 times that of GaAs, while its refractive index is about 20 % lower, the figure of merit for electrooptic modulation, $n_0^3 r_{41}$, is about twice as high for CdTe as for GaAs.

TABLE VII

Electrooptic coefficient and nonlinear susceptibility of CdTe

Electrooptic coefficient, r_{41} (m/V) [a]	
At 10.6 μm	5.2×10^{-12}
At 28.0 μm	5.2×10^{-12}
$n_0^3 r_{41}$ (m/V)	
At 10.6 μm [b]	1.0×10^{-10}
At 28.0 μm [c]	8.5×10^{-11}
Nonlinear susceptibility, d_{14} (m/V)	
At 10.6 μm [d]	$(16.8 \pm 6.3) \times 10^{-11}$
At 28.0 μm [e]	$(5.9 \pm 2.4) \times 10^{-11}$

[a] Calculated from measured values of $n_0^3 r_{41}$ and n_0.
[b] KIEFER, E., NUSSMEIER, T. A. and GOODWIN, F. E., *IEEE J. Quantum Electron.* **QE-8** (1972) 173.
[c] AKITT, D. P., JOHNSON, C. J. and COLEMAN, P. D., *IEEE J. Quantum Electron.* **QE-6** (1970) 496.
[d] PATEL, C. K. N., *Phys. Rev. Lett.* **16** (1966) 613.
[e] SHERMAN, G. H. and COLEMAN, P. D., *J. Appl. Phys.* **44** (1973) 238.

5. **Electrical properties.** — We shall now turn our attention to the electrical properties of CdTe, the last general class of physical properties that will be reviewed in this paper. Like the optical properties, they are ultimately limited by the electronic band structure, which determines the intrinsic carrier concentration, and by the lattice vibration modes, which set upper limits on the electron and hole mobilities. However, the electrical properties are influenced to a much greater extent by impurities, native defects, and the interactions between them.

A semiconductor's intrinsic carrier concentration n_i is determined by three band-structure parameters : the energy gap E_g and the density-of-states effective masses m_n^*/m_0 and m_p^*/m_0 for electrons and holes, respectively. We have used the standard theoretical expression to calculate values of n_i for temperatures between 300 and 1 200 K by adopting the following values for these parameters :

$$E_g\,(\text{eV}) = 1.622 - 3.5 \times 10^{-4}\,\text{T}\,,$$

$m_n^*/m_0 = 0.1$, and $m_p^*/m_0 = 0.8$. The expression for E_g is based on the exciton reflectance data mentioned previously, the electron effective mass approximates the value of 0.0963 obtained by Mears and Stradling [52] from cyclotron resonance data, and the hole effective mass is the heavy-hole mass value that Kranzer [53] found to give the best fit between his theoretical mobility calculations and the experimental data. This choice of parameters leads to the following equation for the intrinsic carrier concentration :

$$n_i^2 = (3.066 \times 10^{31})\,\text{T}^3 \exp(-1.882 \times 10^4/\text{T}).$$

According to this expression, n_i is only 6.9×10^5 cm^{-3} at 300 K and only 1.5×10^{14} cm^{-3} even at 700 K. It is clear that intrinsic carriers do not make an important contribution to conduction at room temperature in any CdTe samples so far prepared, since the lowest room-temperature carrier concentration of which I am aware is 8.3×10^7 cm^{-3}, as reported by Alekseenko *et al.* [54] for a p-type sample. Furthermore, because n_i is so low, mixed conduction due to both electrons and holes does not occur at room temperature. Thus even in the sample just mentioned the electron concentration is so low that less than 0.1 % of the current is carried by electrons, in spite of the fact that they are about 10 times as mobile as holes.

The preceding discussion shows that the current carriers responsible for conduction in CdTe at room temperature and below must be generated by the ionization of impurities, native defects, or complexes between them. Returning to figure 1, the portion of the periodic table shown previously, we see most of the impurity elements that have been identified as electrically active in CdTe. Their observed activity as acceptors or donors can be explained by assuming that elements in the columns adjacent to Cd in the table substitute for Cd atoms in the lattice and those adjacent to Te substitute for Te, then applying the usual rule that a substitutional impurity is a donor or acceptor depending on whether it has more or less valence electrons than the atom it replaces. Since elements in adjacent columns differ by one valence electron, all the impurities considered here should be singly ionized acceptors or donors. (Since the electrical properties of these elements were reviewed at the 1971 Symposium [55], I shall refer explicitly only to investigations reported since then.)

Thus the Group V elements P, As, and Sb are acceptors, presumably substituting for Te. Gu *et al.* [56] have reported the growth from the melt of P-doped crystals with room-temperature hole concentrations of 5×10^{16} to 6×10^{17} cm^{-3} and mobilities of 24 to 39 cm^2 V^{-1} s^{-1}. They measured ionization energies between 0.036 and 0.060 eV, compared with an earlier value of about 0.05 eV obtained for samples with hole concentrations a little above 10^{16} cm^{-3}. The acceptor behavior of As is demonstrated by its ability to convert n-type samples to p-type by ion implantation, but no measurements of its ionization energy have been reported. Höschl and Kubalkova [57] state that highly conducting p-type CdTe can be prepared by Sb doping but give no details.

The Group IB elements Cu, Ag, and Au are also acceptors, presumably substituting for Cd, with ionization energies reported in the range from 0.3 to 0.4 eV. Popova and Polivka [58] have described the preparation of samples with room-temperature hole concentrations as high as 1×10^{18} cm^{-3} and conductivities as high as 90 Ω^{-1} cm^{-1}, the highest so far reported for p-type CdTe, by means of Cu diffusion. They do not give ionization energies, and there appear to be inconsistencies among their tabulated values for conductivity, carrier concentration, and mobility. On the basis of Rutherford backscattering experiments Akutagawa *et al.* [59] report that, depending on annealing conditions, between 50 and 85 % of the Au present in CdTe is substituted on Cd sites, with the rest present either interstitially or in the form of precipitates.

The Group IA elements Na and Li, which are not shown in figure 1, are also acceptors that presumably substitute for Cd. Like P they are shallow acceptors, with reported ionization energies of 0.028 and 0.034 eV, respectively, for samples with room-temperature hole concentrations close to 10^{17} cm^{-3}.

The two types of donor impurities that have been identified in CdTe are both shown on figure 1 : the Group III elements Al, Ga, and In, which presumably substitute for Cd, and the Group VII halogens Cl, Br and I, which presumably substitute for Te. The highest room-temperature carrier concentration that can be obtained by doping with Ga is about 4×10^{17} while concentrations of about 2×10^{18} cm^{-3} can be obtained with the other elements. It has not been possible to determine ionization energies of these impurities because carrier freeze-out with decreasing temperature has not been observed for samples to which a dopant has been added in a sufficient quantity to be identified as the dominant donor. The absence of freeze-out results because the ionization energy of an impurity in a semiconductor decreases as its concentration increases, and shallow donor levels eventually merge with the conduction band at sufficiently high concentrations. This effect is shown by figure 23, which

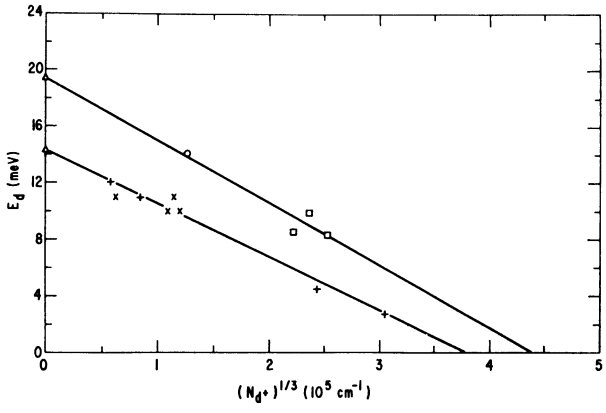

FIG. 23. — Donor ionization energy vs ionized donor concentration for CdS (upper line) and CdTe (lower line) (Woodbury and Aven, Ref. [60]).

is a plot given by Woodbury and Aven [60] for the donor ionization energy E_d in CdSe (upper line) and CdTe (lower line) as a function of the ionized donor concentration N_{d+}. The points for CdTe were obtained by analysis of the Hall coefficient vs temperature data of Agrinskaya *et al.* [61] (crosses) for one nominally Al-doped and three nominally undoped samples and the data of Segall *et al.* [62] (*x*'s) for nominally undoped

samples. The points are fit very well by a straight line whose intercept on the abscissa indicates that the ionization energy vanishes when N_{d+} reaches 5×10^{16} cm^{-3}. The limiting ionization energy given by the intercept on the ordinate is 14.3 meV, the value for the donor ionization energy in high-purity samples obtained from the optical absorption data of Cohn, Larsen, and Lax [63]. This agrees with the value of 14.1 meV calculated for hydrogenic donors in CdTe, showing that the donors in high-purity CdTe are hydrogenic. It is therefore generally assumed that the Group III and Group VII donors in CdTe are also hydrogenic. On the basis of high-pressure and photoconductivity measurements it has been suggested by Iseler *et al.* [64] that Ga, In, Cl, and Br introduce non-hydrogenic levels associated with a higher conduction band, but it would be an understatement to say that this suggestion of so-called non-Γ donors has not been widely accepted.

The purest samples of lightly compensated CdTe so far reported have been obtained by Triboulet and Marfaing [65] from single crystals grown by the vertical zone melting of ingots synthesized by the Bridgman method. The best of these samples have room-temperature carrier concentrations between 1 and 5×10^{13} cm^{-3} and resistivities of 100 to 400 Ω.cm. Their low-temperature carrier mobilities, which will be described later, are the highest reported. It has been estimated that the total concentration of electrically active centers in these crystals is about 10^{14} cm^{-3}.

Since we have mentioned that both hole and electron concentrations exceeding 10^{17} cm^{-3} can be obtained by doping CdTe with shallow acceptors and donors, respectively, it is appropriate to point out that CdTe is unique among the semiconducting II-VI compounds in its ability to exhibit both p-type and n-type bulk conductivity at relatively high levels. The conductivity types of the II-VI compounds are summarized in table I. The only one other than CdTe that can exhibit both conductivity types in bulk samples is the semimetal HgTe, and because of the high ratio of electron to hole mobility and the high intrinsic carrier concentration, even at liquid helium temperature, hole concentrations of the order of 10^{19} cm^{-3} are required in order for more current to be carried by holes than by electrons. For ZnSe, as indicated by placing the letter « p » in parentheses, there is fairly good evidence that thin p-type layers can be produced by diffusion of In followed by annealing in Zn vapor [66] and it has also been reported [67] that p-type material can be formed by Li doping or implantation.

The inability of the II-VI semiconductors other than CdTe to exhibit both p- and n-type conductivity is due to the formation of electrically active native point defects that are associated with deviations from the stoichiometric composition. In a II-VI compound, an excess of the metallic element can be incorporated most simply by means of metal interstitials or non-metal vacancies, while an excess of non-metal can be incorporated by means of non-metal interstitials or metal vacancies. The defects associated with excess metal are generally donors and those associated with excess non-metal are generally acceptors, although there is persuasive evidence for neutral interstitials in a number of the compounds. In those compounds that exhibit only n-type conductivity any impurities that would normally be acceptors are rendered ineffective by the presence of native donors. In addition, donor impurities are fully effective only at the metal-saturated boundary of the compound's homogeneity region ; as the composition is made less metal-rich, as can be accomplished by equilibrating the material with metal vapor at pressures lower than the saturation pressure, the donors are compensated to an increasing extent by native acceptor defects. This process, known as self-compensation, continues until the carrier concentration becomes very low and the resistivity correspondingly high. The analogous phenomena, in reverse, take place for the compounds that exhibit only p-type conductivity.

Although CdTe can exhibit both p- and n-type conductivity, like the other II-VI compounds its electrical properties are strongly affected by native defects, and in particular a very high degree of self-compensation is observed for samples that contain excess donor impurities. Before discussing such samples, however, we shall consider the properties of samples that contain few if any excess donor impurities. These properties are illustrated by figure 24, which shows the carrier concentration data reported by Selim, Swaminathan, and Kröger [68] for samples nominally doped with 5×10^{16} cm^{-3} of Cl that were annealed at 700, 800, and 900 °C under different pressures of Cd vapor. The straight lines labelled *high temperature* are isotherms obtained by *in situ* measurements made at each annealing temperature. The samples are all n-type, with electron concentrations that are proportional to $p_{Cd}^{1/3}$. This pressure dependence shows that the carriers are produced by the ionization of doubly-ionized native donors, but the data do not establish whether these donors are Cd interstitials or Te vacancies. After

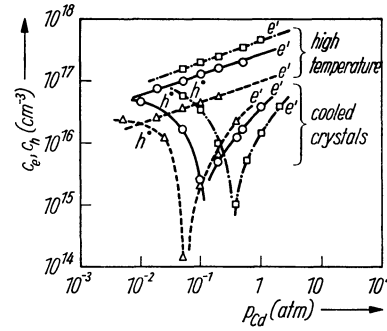

FIG. 24. — Carrier concentration of CdTe vs Cd pressure for samples measured *in situ* or after quenching to room temperature (Selim *et al.*, Ref. [68]).

the samples were cooled to room temperature, those annealed at sufficiently high pressures remained n-type, while those annealed at lower pressures were found to be p-type. Selim *et al.* [68] attribute the holes in the p-type samples to native defects, while Smith [69] has explained similar data in terms of acceptor impurities. In any case, because of the steepness of the concentration-vs-pressure curves near the transition from n- to p-type, it would not be feasible to control the annealing pressure well enough to obtain very low carrier concentrations.

Such low concentrations can be obtained quite readily, however, by utilizing self-compensation in donor-doped samples. The earliest reported example of this effect in CdTe is shown by figure 25, which

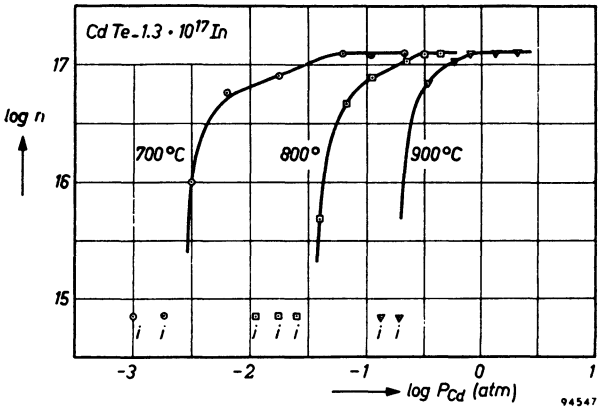

FIG. 25. — Carrier concentration of In-doped CdTe vs Cd pressure for samples measured after quenching to room temperature (de Nobel, Ref. [70]).

gives the data published by de Nobel [70] in 1959 for the carrier concentration measured at room temperature for samples doped with 1.3×10^{17} cm^{-3} In that had been annealed at various Cd pressures at 700, 800, and 900 °C. In each case, when the annealing pressure was reduced below a certain value the carrier concentration dropped abruptly to values too low for de Nobel to measure (represented by points marked « i »), yielding resistivities of 10^6 to 10^7 Ω.cm, and remaining this low no matter how much the Cd pressure was reduced. Similar results have been obtained for samples with donor impurity concentrations as high as 10^{18} cm^{-3}.

Self-compensation has been extensively employed to obtain CdTe samples with carrier concentrations low enough to give the high electrical resistivity needed for γ-ray detectors and the high optical transmission needed for electrooptic modulators and infrared windows. Gentile *et al.* [71] have described a technique for preparing highly transparent samples by annealing material doped with about 2×10^{17} cm^{-3} In over a temperature range down to 700 °C at Te_2 pressures somewhat lower than the saturation pressure. Several other groups have used growth from Te-rich solutions, which yields crystals that are initially Te-saturated at the growth temperature, to establish the deviation from stoichiometry needed for self-compensation. Höschl *et al.* [72] grew Cl-doped crystals by a technique similar to the Bridgman method, while Wald and Bell [73] and Triboulet *et al.* [74] both used the traveling heater method, the former with Cl-doped starting material and the latter with starting material that had been purified by vertical zone melting. Alekseenko *et al.* [54] also used the traveling heater method but doped the crystals with Cl after growth. As mentioned above, they report a carrier concentration of 8×10^7 cm^{-3}, which gave a resistivity of 3×10^{11} Ω.cm. All the Cl-doped semi-insulating crystals grown from Te-rich solutions are p-type.

Numerous localized electronic levels lying within the energy gap of CdTe, many of which undoubtedly involve native defects, have been detected by applying various characterization techniques to high-resistivity CdTe. Since the native defects and the mechanism of self-compensation will be reviewed later in the Symposium by Professor Kröger and Dr. Marfaing, it will not be necessary for this paper to discuss the details of the identification of the localized levels and their influence on the electrical properties of CdTe. It is appropriate, however, to point out the essential role played by deep levels in obtaining semi-insulating properties in any semiconductor. As shown schematically in figure 26,

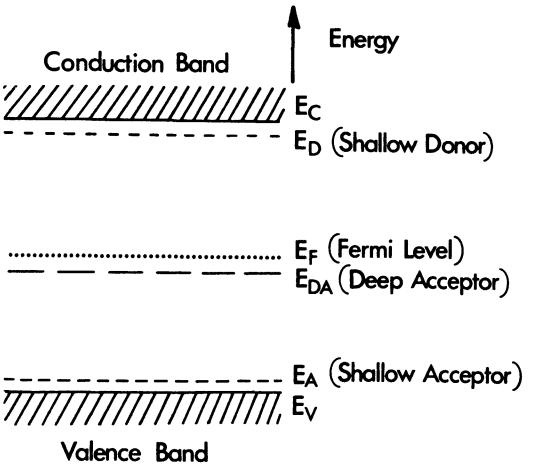

FIG. 26. — Deep-acceptor model for production of semi-insulating, donor-doped semiconductor (Thompson, Ref. [75]).

which is actually taken from a paper by Thompson [75] that discusses the preparation of semi-insulating GaAs, for a material that contains an excess of shallow donors over shallow acceptors the deep levels must be acceptors. When the concentration of deep acceptors becomes high enough to exceed the difference between the shallow donor and acceptor concentrations, the Fermi level will fall abruptly from the vicinity of the shallow donor level to the vicinity of the deep acceptor level, where it remains pinned to yield semi-insulating materials over a wide range of deep acceptor concentrations.

The energies of some of the prominent levels that have been reported to exist within the energy gap of CdTe are shown in figure 27, which reproduces a diagram given by Siffert *et al.* [76]. The level shown

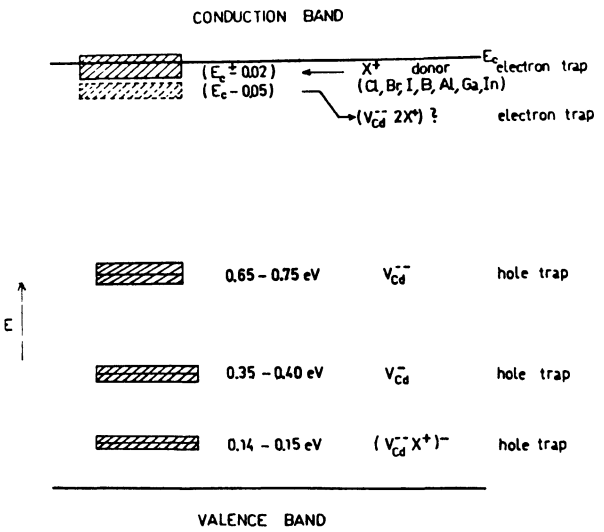

FIG. 27. — Some localized levels within the energy gap of CdTe (Siffert *et al.*, Ref. [76]).

at 0.65-0.75 eV corresponds to the activation energy observed by various workers in resistivity vs temperature measurements on high-resistivity samples. It will be interesting to learn whether the identifications proposed by Siffert *et al.* for the defects responsible for these levels will be generally accepted.

To complete this discussion of the electrical properties of CdTe, we shall now consider the Hall and drift mobilities of electrons and holes. Figure 28 shows the curves of Hall mobility vs temperature reported by Triboulet and Marfaing [65] for n-type samples cut at four locations from the head (curve 1) to the tail

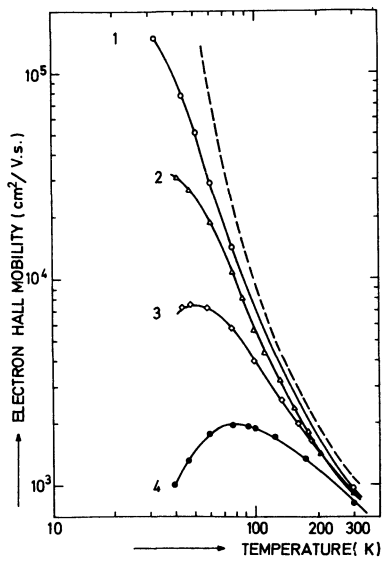

FIG. 28. — Hall mobility vs temperature for electrons in CdTe (Triboulet and Marfaing, Ref. [65]).

(curve 4) of ingots they prepared by vertical zone refining. The impurity content increases systematically from head to tail, as shown by the reduction in mobility at low temperatures due to ionized impurity scattering. The mobility measured for the purest sample at 32 K is 1.46×10^5 cm^2 V^{-1} s^{-1}, the highest reported for CdTe. The data for this sample are in good agreement with the theoretical calculations of Segall, Lorenz, and Halsted [62] represented by the dashed curve, and in even better agreement with the later calculation of Rode [77]. Both theoretical treatments show that polar optical mode scattering is the principal lattice scattering mechanism over the temperature range shown. The mobility measured for sample 1 at 300 K was 950 cm^2 V^{-1} s^{-1}, while other samples that had somewhat lower mobilities at low temperature had mobilities up to 1 100 cm^2 V^{-1} s^{-1} at 300 K.

Figure 29 reproduces a figure given by Triboulet *et al.* [74] for the Hall mobility of holes in CdTe as a

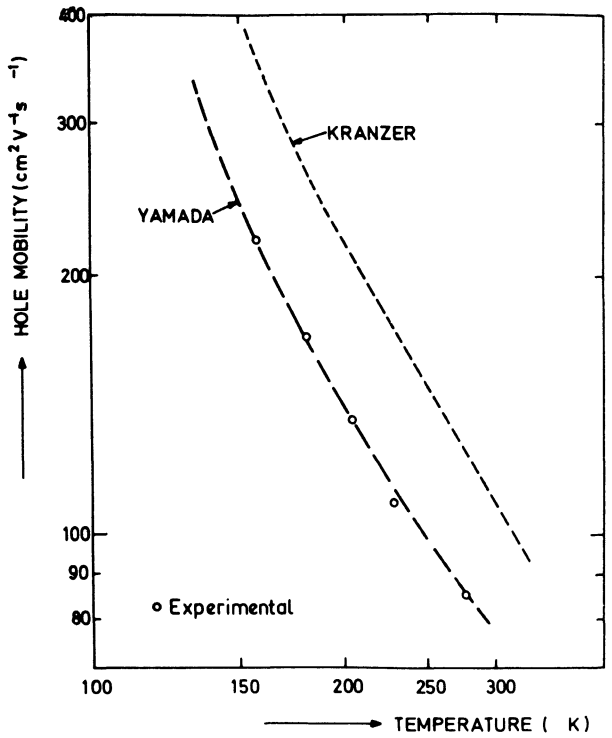

FIG. 29. — Hall mobility vs temperature for holes in CdTe (Triboulet *et al.*, Ref. [74]).

function of temperature. The lower curve is the empirical curve that Yamada [78] fitted to his experimental data for as-grown, nominally undoped p-type samples with room-temperature carrier concentrations of about 5×10^{14} cm^{-3}. The mobility is about 80 cm^2 V^{-1} s^{-1} at 300 K. The curve has the functional dependence expected for optical mode scattering according to the treatment of Low and Pines [79]. The points shown represent the data of Triboulet *et al.* [74] for semi-insulating p-type samples with room-temperature carrier concentrations of about 10^{10} cm^{-3} that were

grown by the traveling heater method from ingots purified by vertical zone melting. The data are in excellent agreement with Yamada's results. The upper curve represents the theoretical calculations of Kranzer [53]. According to these calculations polar optical mode scattering is the dominant scattering mechanism at room temperature, while this mechanism and acoustic deformation potential scattering are equally important at about 100 K. Piezoelectric and optical deformation potential scattering do not significantly affect the mobility over the temperature range shown.

The time-of-flight technique has been used by the Modena group to measure the drift velocities of electrons and holes in semi-insulating CdTe. The smoothed data of Canali *et al.* [80] for electrons are shown in figure 30, where the drift velocity in samples with

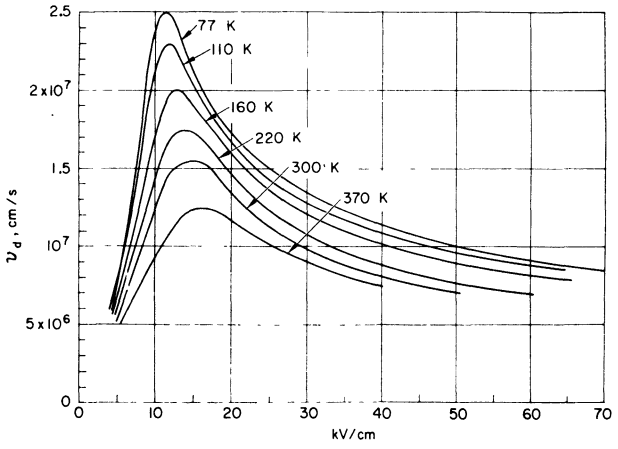

FIG. 30. — Drift velocity vs electric field for electrons in semi-insulating CdTe (Canali *et al.*, Ref. [80]).

resistivities of 10^8 to 10^9 Ω.cm is plotted vs electric field for temperatures between 77 and 370 K. With increasing field the velocity initially increases, reaches a maximum, and then decreases due to the transfer of electrons from the conduction band minimum at Γ to higher minima. At fields below the velocity maximum the drift mobility at room temperature is in good agreement with the Hall mobility due to lattice scattering that is measured for low-resistivity samples.

Figure 31 shows the data of Ottaviani *et al.* [81] for the drift mobility of holes in semi-insulating samples as

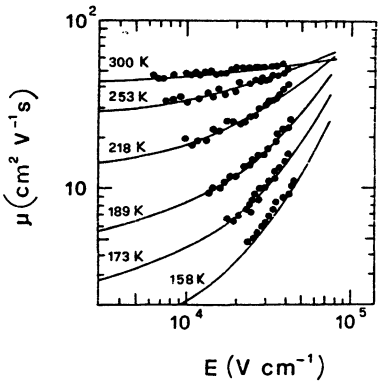

FIG. 31. — Drift mobility vs electric field for holes in semi-insulating CdTe (Ottaviani *et al.*, Ref. [81]).

a function of temperature and electric field. At room temperature the mobility is in fair agreement with the Hall mobility of holes measured on low-resistivity samples, and it does not depend strongly on applied field. With decreasing temperature the drift mobility at fixed field decreases as trapping becomes more important, and it therefore becomes more dependent on field, because the effect of trapping is reduced by the Poole-Frenkel mechanism. The curves shown were calculated from the theory for this mechanism by assuming a trap concentration of 5×10^{16} cm^{-3} and a trap activation energy of 140 meV.

The performance of γ-ray detectors depends critically on the products of mobility and trapping time for electrons and holes. I shall conclude this paper with figure 32, which shows the curves given by Siffert *et al.* [76] for the $\mu\tau$ products over the years from 1966 through 1974. Alekseenko *et al.* [54] have reported values for both electrons and holes — 2.6×10^{-3} and 4×10^{-4} cm^2 V^{-1} — that are significantly higher than the best shown. It will be of interest to learn whether this advance is matched or exceeded by the results to be reported at this Symposium.

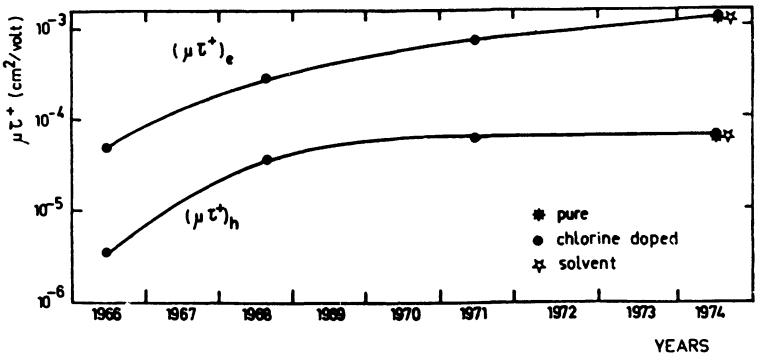

FIG. 32. — Mobility-lifetime products for electrons and holes in CdTe reported from 1966 through 1974 (Siffert *et al.*, Ref. [76]).

References

[1] PHILLIPS, J. C., *Bonds and Bands in Semiconductors* (Academic Press, New York) 1973, p. 42.

[2] HILSUM, C. and ROSE-INNES, A. C., *Semiconducting III-V Compounds* (Pergamon Press, New York) 1961, frontispiece.

[3] INOUE, M., TERAMOTO, I. and TAKAYANAGI, S., *J. Appl. Phys.* **33** (1962) 2578.

[4] SHALIMOVA, K. V., BULATOV, O. S., VORONKOV, E. N. and DIMITRIEV, V. A., *Krist.* **11** (1966) 480 [*Sov. Phys.-Cryst.* **11** (1966) 431].

[5] SPÎNULESCU-CARNARU, I., *Phys. Stat. Sol.* **15** (1966) 761.

[6] CLINE, C. F. and STEPHENS, D. R., *J. Appl. Phys.* **36** (1965) 2869.

[7] YU, W. C. and GIELISSE, P. J., *Mater. Res. Bull.* **6** (1971) 621.

[8] MARIANO, A. N. and WAREKOIS, E. P., *Science* **142** (1963) 672.

[9] SAMARA, G. A. and DRICKAMER, H. G., *J. Phys. Chem. Solids* **23** (1962) 457.

[10] MEDVEDEV, S. A., MAKSIMOVSKII, S. N., KISELEVA, K. V., KLEVKOV, Yu. V. and SENTYURINA, N. N., *Izv. AN SSSR, Neorg. Mater.* **9** (1973) 356 [*Inorg. Mater.* **9** (1973) 321].

[11] VAIPOLIN, A. A. and RUD', Yu. V., *Izv, AN SSSR, Neorg. Mater.* **10** (1974) 550 [*Inorg. Mater.* **10** (1974) 470].

[12] VOHL, P. and WOLFE, C. M., Electronic Materials Conference, Salt Lake City, Utah, June, 1976, paper F 6.

[13] VAIPOLIN, A. A., *Fiz. Tverd. Tela* **15** (1973) 1223 [*Sov. Phys. Solid State* **15** (1973) 823].

[14] WILLIAMS, M. G., TOMLINSON, R. D. and HAMPSHIRE, M. J., *Solid State Commun.* **7** (1969) 1831.

[15] SMITH, T. F. and WHITE, G. K., *J. Phys.* C **8** (1975) 2031.

[16] GREENOUGH, R. D. and PALMER, S. B., *J. Phys.* D **6** (1973) 587.

[17] SLACK, G. A., *Phys. Rev.* B **6** (1972) 3791.

[17A] SOOD, K. C., SINGH, M. P. and VERMA, G. S., *Phys. Rev.* **B 3** (1971) 385.

[17B] HOLLAND, M. G., *Phys. Rev.* **134** (1964) 471.

[18] RUSAKOV, A. P., VEKILOV, Yu. Kh. and KADYSHEVICH, A. E., *Fiz. Tver. Tela* **12** (1970) 3238 [*Sov. Phys.-Solid State* **12** (1971) 2618].

[19] MCSKIMIN, H. J. and THOMAS, D. G., *J. Appl. Phys.* **33** (1962) 56.

[20] VEKILOV, Yu. Kh. and RUSAKOV, A. P., *Fiz. Tver. Tela* **13** (1971) 1157 [*Sov. Phys.-Solid State* **13** (1971) 956].

[21] BERLINCOURT, D., JAFFE, H. and SHIOZAWA, L. R., *Phys. Rev.* **129** (1963) 1009.

[22] SWAMINATHAN, V., SELIM, F. A. and KRÖGER, F. A., *Phys. Stat. Sol.* (a) **30** (1975) 721.

[23] CARLSSON, L. and AHLQUIST, C. N., *J. Appl. Phys.* **43** (1972) 2529.

[24] WALFORD, L. K. and SCHOEFFEL, J. A., *Phil. Mag.* **21** (1970) 375.

[25] ZUBIK, K. and VALVODA, V., *Czech. J. Phys.* B **25** (1975) 1149.

[26] BIRCH, J. A., *J. Phys.* C **8** (1975) 2043.

[27] ROWE, J. M., NICKLOW, R. M., PRICE, D. L. and ZANIO, K., *Phys. Rev.* **B 10** (1974) 671.

[28] PLUMELLE, P. and VANDEVYVER, M., *Phys. Stat. Sol.* (b) **73** (1976) 271.

[29] PERKOWITZ, S. and THORLAND, R. H., *Phys. Rev.* B **9** (1974) 545.

[30] SERREZE, H. B., ENTINE, G., BELL, R. O. and WALD, F. V., *IEEE Trans. Nucl. Sci.* **NS-21** (1974) 404.

[31] SIFFERT, P., GONIDEC, J. P., CORNET, A., BELL, R. O. and WALD, F. V., *Nucl. Instrum. Meth.* **115** (1974) 13.

[32] ALBERIGI QUARANTA, A., CANALI, C., OTTAVIANI, G. and ZANIO, K. R., *Nuovo Cimento Lett.* **4** (1970) 908.

[33] CORNET, A., SIFFERT, P., COCHE, A. and TRIBOULET, R., *Appl. Phys. Lett.* **17** (1970) 432.

[34] CHADI, D. J., WALTER, J. P., COHEN, M. L., PETROFF, Y. and BALKANSKI, M., *Phys. Rev.* B **5** (1972) 3058.

[35] FREEOUF, J. L., *Phys. Rev.* B **7** (1973) 3810.

[36] MARPLE, D. T. F., *Phys. Rev.* **150** (1966) 728.

[37] THOMAS, D. G., *J. Appl. Phys.* **32** (Supp.) (1961) 2298.

[38] See SEGALL, B., *Phys. Rev.* **150** (1966) 734.

[39] CAMASSEL, J., AUVERGNE, D., MATHIEU, H., TRIBOULET, R. and MARFAING, Y., *Solid State Commun.* **13** (1973) 63.

[40] LOFERSKI, J. J., *J. Appl. Phys.* **27** (1956) 777.

[41] BABONAS, G. A., BENDORYUS, R. A. and SHILEIKA, A. Yu., *Fiz. Tekh. Poluprov.* **5** (1971) 449. [*Sov. Phys.-Semicond.* **5** (1971) 392.

[42] MELZ, P. J. and ORTENBURGER, I. B., *Phys. Rev.* B **3** (1971) 3257.

[43] STRAUSS, A. J. and ISELER, G. W., *Bull. Am. Phys.* **17** (1972) 326.

[44] JENSEN, B., *J. Phys. Chem. Solids* **34** (1973) 2235.

[45] VUL, B. M., SAL'MAN, V. M. and CHAPNIN, V. A., *Fiz. Tekh. Poluprov.* **4** (1970) 67 [*Sov. Phys.-Semicond.* **4** (1970) 52].

[46] CAPEK, V., ZIMMERMAN, K., KONAK, C., POPOVA, M. and POLIVKA, P., *Phys. Stat. Sol.* (b) **56** (1973) 729.

[47] DEUTSCH, T. F., *J. Phys. Chem. Solids* **34** (1973) 2091.

[48] MAGEE, T. J., PENG, J. and BEAN, J., *Phys. Stat. Sol.* (a) **27** (1975) 557.

[49] STAFSUDD, O. M., HAAK, F. A. and RADISAVLJEVIĆ, K., *J. Opt. Soc. Amer.* **57** (1967) 1475.

[50] DANIELEWICZ, E. J. and COLEMAN, P. D., *Appl. Opt.* **13** (1974) 1164.

[51] MANABE, A., MITSUISHI, A. and YOSHINAGA, H., *Japan J. Appl. Phys.* **6** (1967) 593.

[52] MEARS, A. L. and STRADLING, R. A., *Solid State Commun.* **7** (1969) 1267.

[53] KRANZER, D., *J. Phys.* C **6** (1973) 2977.

[54] ALEKSEENKO, M. V., ARKAD'EVA, E. N., KISILENKO, V. S., MASLOVA, L. V., MATVEEV, O. A., PROKOF'EV, S. V., RYVKIN, S. M. and KHUSAINOV, A. Kh., *Fiz. Tekh. Poluprov.* **8** (1974) 550 [*Sov. Phys.-Semicond.* **8** (1974) 351].

[55] STRAUSS, A. J., *Proc. Int. Sym. on Cadmium Telluride*, Strasbourg, 1971 (P. Siffert and A. Cornet, Eds.), paper I.

[56] GU, J., KITAHARA, T., KAWAKAMI, K. and SAKAGUCHI, T., *J. Appl. Phys.* **46** (1975) 1184.

[57] HÖSCHL, P. and KUBÁLKOVÁ, S., *Czech. J. Phys.* **B 22** (1972) 530.

[58] POPOVA, M. and POLIVKA, P., *Czech. J. Phys.* B **23** (1973) 110.

[59] AKUTAGAWA, W., TURNBULL, D., CHU, W. K. and MAYER, J. W., *J. Phys. Chem. Solids* **36** (1975) 521.

[60] WOODBURY, H. H. and AVEN, M., *Phys. Rev.* B **9** (1974) 5195.

[61] AGRINSKAYA, N. V., ARKAD'EVA, E. N. and MATVEEV, O. A., *Fiz. Tekh. Poluprov.* **5** (1971) 863 [*Sov. Phys.-Semicond.* **5** (1971) 762].

[62] SEGALL, B., LORENZ, M. R. and HALSTED, R. E., *Phys. Rev.* **129** (1963) 2471.

[63] COHN, D. R., LARSEN, D. M. and LAX, B., *Solid State Commun.* **8** (1970) 1707.

[64] ISELER, G. W., KAFALAS, J. A., STRAUSS, A. J., MACMILLAN, H. F. and BUBE, R. H., *Solid State Commun.* **10** (1972) 619.

[65] TRIBOULET, R. and MARFAING, Y., *J. Electrochem. Soc.* **120** (1973) 1260.

[66] KUN, Z. K. and ROBINSON, R. B., *Electron. Mater.* **5** (1976) 23.

[67] PARK, Y. S., HEMENGER, P. M. and CHUNG, C. H., *Appl. Phys. Lett.* **18** (1971) 45 ;
PARK, Y. S. and CHUNG, C. H., *Appl. Phys. Lett.* **18** (1971) 99.

[68] SELIM, F. A., SWAMINATHAN, V. and KRÖGER, F. A., *Phys. Stat. Sol.* (a) **29** (1975) 465.

[69] SMITH, F. T. J., *Met. Trans.* **1** (1970) 617.
[70] DE NOBEL, D., *Philips Res. Repts* **14** (1959) 361.
[71] GENTILE, A. L., KIEFER, J. E., KYLE, N. R. and WINSTON, H. V., *Mater. Res. Bull.* **8** (1973) 523.
[72] HÖSCHL, P., POLIVKA, P., PROSSER, V. and SAKALAS, A., *Czech. J. Phys.* **B 25** (1975) 585.
[73] WALD, F. V. and BELL, R. O., *Nature Phys. Sci.* **237** (1972) 13.
[74] TRIBOULET, R., MARFAING, Y., CORNET, A. and SIFFERT, P., *J. Appl. Phys.* **45** (1974) 2759.
[75] THOMPSON, A. G., *J. Electron. Mater.* **2** (1973) 47.
[76] SIFFERT, P., CORNET, A., STUCK, R., TRIBOULET, R. and MARFAING, Y., *IEEE Trans. Nucl. Sci.* **NS-22** (1975) 211.
[77] RODE, D. L., *Phys. Rev.* **B 2** (1970) 4036.
[78] YAMADA, S., *J. Phys. Soc. Japan* **15** (1960) 1940.
[79] LOW, F. and PINES, D., *Phys. Rev.* **98** (1955) 414.
[80] CANALI, C., MARTINI, M., OTTAVIANI, G. and ZANIO, K. R., *Phys. Rev.* **B 4** (1971) 422.
[81] OTTAVIANI, G., CANALI, C. and ALBERIGI QUARANTA, A., *IEEE Trans. Nucl. Sci.* **NS-22** (1975) 192.